Managing Flexibility in Multi-Area Power Systems

Matthias A. Bucher, *Student Member, IEEE*, Spyridon Chatzivasileiadis, *Member, IEEE*, and Göran Andersson, *Fellow, IEEE*

***Abstract*—In this paper we present a framework to efficiently characterize the available operational flexibility in a multi-area power system. We focus on the available reserves and the tie-line flows. The proposed approach is an alternative to the current calculation of the available transfer capacity (ATC), as it considers location and availability of reserves, transmission constraints, and interdependencies of tie-line flows between different areas, while it takes into account the $\mathrm{N}-1$ security criterion. The method is based on computational geometry using polytopic projections. It requires only a limited amount of information exchange and does not need central coordination. The method has two versions: a passive approach, and an active approach where neighboring areas can share reserves. In that respect we also introduce the term "exportable flexibility". Case studies demonstrate the improved tie-line utilization, especially if reserves are shared, and the visualization benefits.**

***Index Terms*—Computational geometry, inter-TSO coordination, operational flexibility.**

I. Introduction

POWER systems in Europe, as well as in other parts of the world, are undergoing fundamental changes. First, increasing shares of fluctuating renewable energy sources are connected to the network. Second, electricity markets are becoming larger covering wider areas. In Europe, for example, regional markets are merged towards a common European energy exchange [1]. These developments result in more frequent power flow changes and higher power transfers which stretch over longer distances. Substantial network reinforcements are often essential to accommodate such flows and ensure power system security [2]. However, long licensing procedures for building new lines, increased public opposition and high investment costs call for additional measures to tackle the emerging problems. Besides building additional lines, flexibility in power system can be achieved by fast-reacting power sources, flexible loads, and a better utilization of the transmission line infrastructure. This paper will focus on the computation of the cross-border transmission line limits, to increase power system flexibility and account for the contribution of flexible resources in neighboring areas to deal with contingencies occurring in the area in question. In order to properly account for the interdependencies between cross-border available transmission capacities and the flexible resources in each area, a centralized computation seems as the most straightforward approach. Transmission system operators (TSOs), as for example in Europe, are currently operating the control reserves in different control areas mainly independently and without coordination. It should be noted, nevertheless, that first steps towards an improved coordination have been taken in countries such as Germany where the procurement and operation of reserves of the four TSOs has been merged. Furthermore, the establishment of bodies such as TSC, a cooperation initiative between thirteen European TSOs, and CORESO, which acts as a coordination service center with the objective to enhance the level of security of supply in Europe, are further initiatives addressing the aforementioned challenges in the European context.

Numerous definitions of flexibility exist [3]. For the scope of this paper we define *operational flexibility* as follows:

Definition 1: The operational flexibility of a system is the ability of the system to react to a disturbance sufficiently fast in order to keep the system secure. A disturbance can either be a component outage, e.g., a line, generator, or a deviation of power injection, e.g., due to forecast errors.

Main sources of flexibility are generation sources, which are usually contracted to provide regulating energy (spinning reserves) or are able to be redispatched sufficiently fast (manual reserves). Besides generation however, switching operations, demand response, electricity storage, and the power flow controllability of new components such as HVDC lines can also provide a significant source of flexibility (for HVDC, see, e.g., [4]). A metric to quantify available operational flexibility in terms of available energy, power capacity and up- and down ramping is for example introduced by the authors in [5].

Flexibility in a power system's context has been discussed in various publications. For example, the authors of [6] present a polytope-based method in order to represent the operational limits over time. The aggregation of multiple units can be found as a Minkowski summation as long as no transmission constraints are imposed. In [7] a method to estimate the probability of insufficient ramping capabilities is presented and [8] tries to optimize the flexibility of a generation mix.

In this paper we focus on the coordination of flexibility *between* TSOs and on inter-TSO flows. Envisioned is an operation paradigm, where TSO A communicates the boundaries of allowed power flow deviations on the tie-lines to TSO B, taking into account the available reserves in its own area. TSO B can use this information when it needs additional flexibility: for example, it can deviate from the agreed tie-line flows, knowing

Manuscript received August 28, 2014; revised December 19, 2014; accepted March 07, 2015. This work was carried out within the project Balancing Power in the European System (BPES) and supported by the Swiss Federal Office of Energy (SFOE) and Swissgrid. Paper no. TPWRS-01174-2014.

M. A. Bucher and G. Andersson are with the EEH-Power Systems Laboratory, Department of Information Technology and Electrical Engineering, ETH Zurich, Zurich, Switzerland (e-mail: mb@eeh.ee.ethz.ch; andersson@eeh.ee.ethz.ch).

S. Chatzivasileiadis is with Lawrence Berkeley National Laboratory, Berkeley, CA 94720 USA (e-mail: schatzivasileiadis@lbl.gov).

Color versions of one or more of the figures in this paper are available online at http://ieeexplore.ieee.org.

Digital Object Identifier 10.1109/TPWRS.2015.2413387

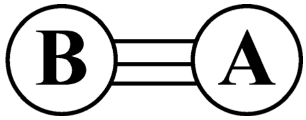

Fig. 1. Two-area system.

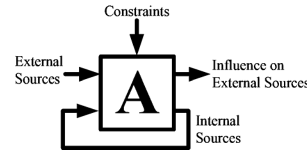

Fig. 2. MIMO system.

that TSO A will be able to act correctively to handle any contingencies occurring in area A from the tie-line flow change. At the same time, TSO B communicates the calculated boundaries for the tie-line flow deviations to TSO A, taking into account the available reserves in area B. In this way, TSO B guarantees that it can take the necessary control actions which will ensure a secure operation in TSO A's control area. Both such actions deal with flexibility offered to the neighboring area in order to ensure a secure power system operation. Therefore we introduce and define the term *exportable flexibility*:

Definition 2: The exportable flexibility, is the operational flexibility originating in a control area that can be used by neighboring control areas. In essence, exportable flexibility corresponds to the amount of reserves that one TSO is able to offer to the neighboring TSO transmitting it over the tie-lines.

In Section VI, the range of exportable flexibility is quantified.

The main contributions of this paper are threefold: First, flexibility metrics in literature are determined focusing mainly on flexibility of units, while no transmission constraints are assumed within or between control areas, i.e., "copperplate approach". Limited transmission capacity leads to flexibility availabilities that are different in different locations in the grid. We present a method for multiple areas taking into account the inter- and intra-area transmission constraints and their interdependencies. The metric used in this paper could possibly be used to extend other metrics such as in [5]. Further, the metric in this paper only describes the available flexibility that can be activated by suitable control actions at certain points in the grid, in terms of available power. It does not give an indication of whether this available flexibility is adequate, for instance, if the ramping capabilities are sufficient [7]. Second, the approach is decentralized, not requiring any central coordination, i.e., the TSOs exchange the relevant information bilaterally. Therefore, it can be applied to the current operation paradigm. Third, exploiting spatial information about the contracted reserves, i.e., assuming that the TSO knows the location of the contracted reserves in its area, we show that the tie-line utilization can be improved compared with the current usual calculation of the Available Transmission Capacity (ATC). The ATC currently reflects the maximum tie-line flow which can be exchanged between two areas, without leading to any contingencies to any of the two areas. The ATC calculation is conservative, as it has no spatial information about the location of the reserves and always assumes the worst case.

The method is based on computational geometry and has several advantages and features. First, through the use of polytopic projections, only the limits on the interconnecting power flows are communicated between the TSOs. No explicit information pertaining to potentially confidential data, such as the grid topology, committed generators or reserve availability need to be exchanged. Taking further advantage of computational geometry techniques, the proposed method also allows a straightforward visualization of the resulting flexibility metric.

In the method, we distinguish between two alternatives: an *active approach*, where corrective control measures are allowed, and a *passive approach*, where no corrective control measures are used. Both approaches consider spatial information concerning the nodes to which power will be injected, and the corresponding anticipated power flow changes. The *passive approach* leads to a set of possible combinations of power flow deviations on the tie-lines without causing congestions. The *active approach* extends the passive approach by enabling the sharing of reserves between the control areas. Therefore the range of possible tie-line flows is larger, as we assume that if TSO B incurs changes to the tie-line flows between areas A and B, TSO A is able to carry out the necessary corrective control actions in area A to avoid any contingencies. The tie-line utilization for reserve operation compared to current ATC calculation is therefore improved.

The remainder of this paper is structured as follows: In Section II we define the problem. In Section III we formulate the equations describing the available flexibility and in Section IV we build the flexibility sets for the active and passive approach. Section V presents the proposed method for computing the limits on the deviations of the tie-line flows. The performance of this method is investigated in a case study in Section VI. Section VII concludes the paper and gives an outlook for future research.

II. Definition of the Problem and Approach

In this paper, we consider a power system, divided in two control areas where tie-lines (AC and DC) form the interconnection between the two neighboring areas. For brevity and clarity we focus on two control areas. The generalization to more than two areas is presented in Section V-C. Fig. 1 shows the two control areas A and B. Each area is assumed to be controlled by an individual TSO. The power flows on the tie-lines are influenced by the unit commitment and dispatch in both regions.

The method should provide the limits on the tie-lines considering the limits of flexible resources in area A which could assist area B in case of a disturbance, and vice-versa.

As shown in Fig. 2, control area A can be further abstracted as a system with multiple inputs and multiple outputs (MIMO system). We distinguish between *external sources* and *internal sources*. External sources are inputs that can directly be influenced by neighboring areas such as flows on tie-lines or HVDC interconnections. Internal sources are controlled locally, e.g., generation units within area A. This MIMO system is subject to constraints, such as intra-area transmission capacity limits and generation capacities. Internal sources can provide remedial measures to correct the impact of external sources, e.g., avoid overloading of transmission lines.

Ultimately, the goal of this work is to find the set of allowed setpoint combinations of external sources, for which possibly needed corrective control measures are available, such that all the operational constraints are satisfied.

III. Quantification of Flexibility

The available flexibility depends on the current system state, i.e., the dispatch. We assume that the dispatch is given, i.e., the generation units are injecting active power at setpoints given by the vector P_{gen} such that the demand P_{load} is covered and operational constraints are respected. The net injections per bus $P_{\text{Bus}} = P_{\text{gen}} - P_{\text{load}}$ lead to power flows P_L that have to remain within transmission limits $[\underline{P}_L, \overline{P}_L]$.

This could be considered as the outcome of a market operation. In order to guarantee a secure operation, the N − 1 security criterion is commonly used to make sure that the outage of a single element does not lead to a blackout. The given dispatch is required to fulfill the N − 1 criterion.

A. Power Flows Per Area and Δ-Notation

We split the system into two control areas as in Section II and distinguish for every control area the contribution to the power flows caused by *internal* sources and *external* sources.

As shown in (1), the power flows can be split into scheduled flows P_L^{sched} and deviations P_L^{dev}. The scheduled flows are based on a given generation dispatch, which could for example be considered as the result of a market clearing. They are calculated using the full AC power flow equations. The deviations P_L^{dev} are determined using the power transfer distribution factor (PTDF) matrix. The PTDF matrix describes the sensitivity H_{jb} of a specific power flow $P_{L,j}$ on line j with respect to a change of the net power injection $P_{\text{Bus},b}$, i.e., the difference between total generation and the total load at bus b. In order to maintain the active power balance, the corresponding power is extracted at the reference bus [9]. The PTDF matrix H for the considered area can be split into $[H_i \; H_e]$ where the indices i denote the influence of n_i internal sources and e for n_e external sources on the power flows of the considered area.

The net bus injections can be split into injections from internal and injections from external sources: $P_{\text{Bus}} = [P_{\text{Bus},i} \; P_{\text{Bus},e}]^T$ and further, they can be split into the scheduled power injections $P_{\text{Bus,sched}}$ and deviations p, i.e., $P_{\text{Bus}} = P_{\text{Bus}}^{\text{sched}} + p$.

Altogether, the power flows are written as

$$P_L = P_L^{\text{sched}} + P_L^{\text{dev}} = P_L^{\text{sched}} + H_e p_e + H_i p_i. \tag{1}$$

The selection of the sensitivity approach is motivated by different reasons. First, the deviations are assumed comparably small compared to the total power flows, as the considered time interval ranges from 15 min to 1 h. As a result, PTDFs are assumed to be valid local approximations around the scheduled power flows. Second, the linearized power flow equations are widely used in practice. This helps maintain our problem linear which is beneficial in different aspects, e.g., the integration in optimization problems. There are different ways to account for larger deviations. In practice, several TSOs would set lower power flow limits to ensure that the solution of the linearized equations is feasible. Another approach is to evaluate the feasibility of the proposed remedial action by using the full AC power flow equations. In [10], we proposed linear current distribution factors based on the full AC power flow equations. If we aim for increased accuracy, the approach proposed in this paper could easily be extended to use current distribution factors, account for the tie-line current limits, and approximate the (apparent) power flow deviations of the flexible sources.

For given scheduled flows, we can quantify the remaining transmission capacity for each line until a constraint becomes binding. The remaining transmission capacity is calculated as the difference to the capacity, i.e., $\Delta\underline{P}_L = \underline{P}_L - P_L^{\text{sched}}$ and $\Delta\overline{P}_L = \overline{P}_L - P_L^{\text{sched}}$, respectively.

The allowed changes in the power output at every bus are given by the allowed changes to the schedule, i.e., $\Delta\underline{P}_{\text{Bus}} = P_{\text{res}}^{\text{dn}}$ and $\Delta\overline{P}_{\text{Bus}} = P_{\text{res}}^{\text{up}}$, respectively. $P_{\text{res}}^{\text{dn}}, P_{\text{res}}^{\text{up}}$ are vectors with the maximum changes to the operation setpoint of the generators that the TSO is allowed to make within a specific timeframe, e.g., 15 min. These changes could either be available manual reserves or redispatch measures. The variables $P_{\text{res}}^{\text{dn}}, P_{\text{res}}^{\text{up}}$ incorporate possible dead times and ramping limitations of the redispatched units.

For the remainder of this paper, we only consider the deviations of the setpoints in the vectors p_i, p_e and the corresponding limits written in the Δ-notation, i.e., $\Delta\underline{P}_L$, $\Delta\overline{P}_L$, $\Delta\underline{P}_{\text{Bus}}$ and $\Delta\overline{P}_{\text{Bus}}$.

In the next step we quantify the flexibility by formulating the limits on possible combinations of deviations of internal and external sources. The resulting inequality constraints will be combined in a set that we refer to as *flexibility set*.

B. Constraints for Nominal Operation

We consider first the constraints that have to be satisfied during normal operation, i.e., without any outages. We refer to this as the *N-secure* case. The deviations of the net injections have to be within the allowed changes of the power flow on the transmission lines:

$$\Delta\underline{P}_L \le [\,H_i \quad H_e\,] \begin{bmatrix} p_i \\ p_e \end{bmatrix} \le \Delta\overline{P}_L. \tag{2}$$

The changes of the bus injections have to meet the generation capacities. I is a unity matrix:

$$\Delta\underline{P}_{\text{Bus}} \le \begin{bmatrix} I_i & 0 \\ 0 & I_e \end{bmatrix} \begin{bmatrix} p_i \\ p_e \end{bmatrix} \le \Delta\overline{P}_{\text{Bus}}. \tag{3}$$

The power balance has to be fulfilled, i.e., the sum of the deviations has to be zero. We can rewrite every equality constraint by two inequality constraints. $\mathbf{1}$ is a row vector of ones:

$$[\mathbf{1}_{1\times n_i} \; \mathbf{1}_{1\times n_e}] \begin{bmatrix} p_i \\ p_e \end{bmatrix} = 0 \Leftrightarrow 0 \le [\mathbf{1}_{1\times n_i} \; \mathbf{1}_{1\times n_e}] \begin{bmatrix} p_i \\ p_e \end{bmatrix} \le 0. \tag{4}$$

C. N − 1 *Security Constraints*

In the N − 1 secure case we consider additional constraints for every single line outage and generation unit outage using the generalized generation distribution factor (GGDF) [11] and line outage distribution factor (LODF) [9] matrices. GGDF gives the changes of the line power flows for an outage of a generation unit $P_{\text{gen},k}$. In this paper, it is assumed that the lack of power is distributed on the remaining generators relative to their total capacity. This could be interpreted as the obligation of primary control reserve provision. G is the GGDF matrix where

$G_{jk}P_{\text{gen},k}$ is the change on line j for the outage of generation unit k that produced $P_{\text{gen},k}$ before [11]. The LODF matrix gives the changes of power flows on the lines in the case of a line outage. L is the LODF matrix where $L_{jh}P_{L,h}$ is the change of line flows on line j when line h, carrying $P_{L,h}$, trips [9]. This adds additional constraints for every outage, but the number of constrained variables is not increased. Usually most of the constraints are not binding and can thus be removed.

We consider every possible outage in the set $\mathcal{G}$ of every single generator k:

$$Q_k \begin{bmatrix} p_i \\ p_e \end{bmatrix} + G_k P_{\text{gen},k} \le \Delta \overline{P}_L \quad \forall k \in \mathcal{G}$$
$$Q_k \begin{bmatrix} p_i \\ p_e \end{bmatrix} - G_k P_{\text{gen},k} \ge \Delta \underline{P}_L \quad \forall k \in \mathcal{G}. \tag{5}$$

Further, the line outages in the set $\mathcal{L}$ are considered as

$$R_j \begin{bmatrix} p_i \\ p_e \end{bmatrix} + L_j P_{L,j}^{\text{sched}} \le \Delta \overline{P}_L \quad \forall j \in \mathcal{L}$$
$$R_j \begin{bmatrix} p_i \\ p_e \end{bmatrix} - L_j P_{L,j}^{\text{sched}} \ge \Delta \underline{P}_L \quad \forall j \in \mathcal{L}. \tag{6}$$

The matrices Q and R are defined as

$$\begin{aligned} Q_k &= [\, Q_{i,k} \quad Q_{e,k} \,] \\ &= [\, H_{i,\{c<k\}} \quad H_{i,\{c=k\}} + G_k \quad H_{i,\{c>k\}} \quad H_e \,] \\ R_j &= [\, R_{i,j} \quad R_{e,j} \,] = L_j \, [\, H_{i,\{r=j\}} \quad H_{e,\{r=j\}} \,] \end{aligned} \tag{7}$$

where c, r denote the cth column and the rth row and G_k and L_j are the kth and jth column of the corresponding matrix.

D. Representation in Matrix Form

The constraints (2)–(6) can be written as a matrix inequality of the form $C_i p_i + C_e p_e \le b$. The matrix C_i relates to the internal sources and C_e to external sources. The limits are given by the vector b. The constraints in (2)–(4) represent the constraints for nominal operation. The equations can be compiled to

$$C_{i,N} p_i + C_{e,N} p_e \le b_N. \tag{8}$$

Analogously, the constraints related to $\mathrm{N}-1$ security [(5), (6)] are stacked to

$$C_{i,N-1} p_i + C_{e,N-1} p_e \le b_{N-1}. \tag{9}$$

The matrices $C_{i,N}, C_{e,N}$ and vector b_N are given by

$$\begin{aligned} C_{i,N} &= \left[H_i^T, -H_i^T, [I_i \ 0]^T, [-I_i \ 0]^T, \mathbf{1}_{n_i\times 1}, \mathbf{1}_{n_i\times 1}\right]^T \\ C_{e,N} &= \left[H_e^T, -H_e^T, [0 \ I_e]^T, [0 \ -I_e]^T, \mathbf{1}_{n_e\times 1}, \mathbf{1}_{n_e\times 1}\right]^T \\ b_N &= \left[\Delta \overline{P}_L^T, -\Delta \underline{P}_L^T, \Delta \overline{P}_{\text{Bus}}^T, -\Delta \underline{P}_{\text{Bus}}^T, 0, 0\right]^T. \end{aligned} \tag{10}$$

The matrices $C_{i,N-1}, C_{e,N-1}$ and vector b_{N-1} are given by

$$\begin{aligned} &\forall k \in \mathcal{G}, j \in \mathcal{L}: \\ C_{i/e,N-1} &= \left[Q_{i/e,k}^T, -Q_{i/e,k}^T, R_{i/e,j}^T, -R_{i/e,j}^T\right]^T \\ b_{N-1} &= [(\Delta \overline{P}_L - G_k P_{\text{gen},k})^T, (-\Delta \underline{P}_L - G_k P_{\text{gen},k})^T, \\ &\quad (\Delta \overline{P}_L - L_j P_{L,j}^{\text{sched}})^T, (-\Delta \underline{P}_L - L_j P_{L,j}^{\text{sched}})^T]^T. \end{aligned} \tag{11}$$

IV. Flexibility Sets

The matrix inequalities above define a set which describes all possible combinations of deviations that are feasible. This set is referred to as the *flexibility set*. We formulate the flexibility set for an *active* and a *passive* approach as well as for the N and the $\mathrm{N}-1$ secure case, as will be shown below.

For the flexibility set of the *active approach*, we allow generation units to adapt their operation point, i.e., the TSO uses the flexibility at his disposal in order to react on tie-line flow changes. For the flexibility set of the *passive approach* the TSO does not react on tie-line flow changes.

A. Flexibility Set for Active Approach

The deviations of external sources together with a corresponding reaction of internal sources that are feasible form the *active flexibility set*.

In the nominal case (*Active/N*):

$$F = \{(p_i, p_e) \in \mathbb{R}^{n_i} \times \mathbb{R}^{n_e} | \ldots \quad C_{i,N} p_i + C_{e,N} p_e \le b_N\}. \tag{12}$$

In the $\mathrm{N}-1$ secure case (*Active/N-1*):

$$F = \left\{(p_i, p_e) \in \mathbb{R}^{n_i} \times \mathbb{R}^{n_e} | \ldots \quad \begin{bmatrix} C_{i,N} \\ C_{i,N-1} \end{bmatrix} p_i + \begin{bmatrix} C_{e,N} \\ C_{e,N-1} \end{bmatrix} p_e \le \begin{bmatrix} b_N \\ b_{N-1} \end{bmatrix}\right\}. \tag{13}$$

As the $\mathrm{N}-1$ criterion is incorporated via (5) and (6), the allowed deviations are constrained such that an outage in the considered region can happen without causing $\mathrm{N}-1$ violations.

B. Flexibility Set for Passive Approach

A special case of the active approach is when $p_i = 0$ and thus the internal sources are not deviating from the setpoints, i.e., the generation units are producing according to their initial dispatch. We call this special case the passive approach, as the resulting feasible deviations of the external sources do not lead to any local congestions.

By setting $p_i = 0$, the *passive flexibility set* in the nominal case (*Passive/N*) becomes

$$F = \{p_e \in \mathbb{R}^{n_e} | C_{e,N} p_e \le b_N\}. \tag{14}$$

In the $\mathrm{N}-1$ secure case (*Passive/N-1*):

$$F = \left\{p_e \in \mathbb{R}^{n_e} | \begin{bmatrix} C_{e,N} \\ C_{e,N-1} \end{bmatrix} p_e \le \begin{bmatrix} b_N \\ b_{N-1} \end{bmatrix}\right\}. \tag{15}$$

This defines sufficient margins on the transmission lines in the case of an outage.

V. Methodology and Applications

A. Methodology

The flexibility set F defines the allowed deviations from the current system state. In order to minimize the information and conceal internal data, the desired outcome is a *reduced* set of constraints only depending on the deviations of the tie-line flows, i.e., what combinations of setpoints for the external sources are safe. In the examples to follow, by external sources we always mean the tie-line flows. Depending on the selected

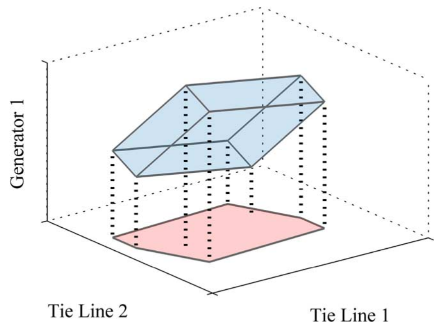

Fig. 3. Projection represents the feasible set for the external sources.

external input, there may be internal adaptation of generation setpoints needed. To better illustrate the methodology, we consider the flexibility set depicted as a blue polytope in Fig. 3 as an example. The system considered consists of two external sources, e.g., two tie-lines, and one internal, e.g., a generator that can be redispatched.

Every feasible setpoint for external sources F_e is then given by the red set, which is the projection of F on the plane spanned by the external sources. Thus, determining F_e is equivalent to calculating the projection of F on the dimensions related to the external sources. Or in other words, a setpoint for the two external sources is feasible, if we can adjust the internal sources such that the resulting operating point is within the flexibility set. In this example we consider only one internal source. In the general case, the number of internal sources n_i corresponds to units that can be redispatched and the number of external sources n_e relates to the number of tie-lines. F_e can be written as

$$\begin{aligned} F_e &= \{p_e \in \mathbb{R}^{n_e} \mid \exists\, p_i, (p_i, p_e) \in F\} \\ &= \{p_e \in \mathbb{R}^{n_e} \mid G p_e \leq g\}. \end{aligned} \tag{16}$$

Area F_e will differ between the active and the passive approach. The F_e of the passive approach is a subspace of the F_e of the active approach. As long as setpoint deviations are within the set F_e of the passive approach, no congestions occur and thus no redispatch is necessary. For deviations in the set of the active approach, which are not in the passive set, the TSO has to adjust the setpoints of selected generation units with respect to the violated operational constraint.

The outcome of the projection is a linear matrix inequality $Gp_e \leq g$ which spans the set of allowed combinations of deviations of the external sources. The number of rows of G is problem dependent and the number of columns is n_e. The linear matrix inequality F_e is communicated to the neighboring TSO. The information gives the neighboring TSO the bounds of possible tie-line flow deviations but does not disclose potentially confidential data to the neighboring TSO, e.g., the generation dispatch of the local control area.

As the polytopes F_e, and F, are bounded by half spaces, i.e., by linear matrix inequalities, the resulting polytopes are always convex. This property allows to directly integrate the bounds in a linear optimization problem as well as it guarantees that we can move from one feasible operating point inside the polytope to another feasible point through a direct path and always staying inside the feasible space.

We use the Multi-Parametric Toolbox which implements the *Equality Set Projection* algorithm the for the calculation of the projections [12]. Due to the limited space in this paper, for more information on the algorithm, the reader is referred to [13]. The calculations presented in the case study are done within a computing time of around 10 s on a standard desktop computer. Future work will investigate the factors influencing the computing time as well possibilities to reduce the problem complexity.

B. Example of Application

The information $Gp_e \leq g$ could be exchanged between the TSOs on a regular basis, e.g., every 15 min, or every hour after the market clearing, or event-based, e.g., when the tie-line flows change substantially. The exchange could happen bilaterally between the TSOs or over a centralized data exchange. It should be noted, that the TSO of every area controls the amount of his (manual) reserves and redispatch capabilities he shares with the neighboring TSOs by including only the offered reserves in the calculation of the flexibility set. We briefly sketch below an example how the information could be used.

We consider TSO B who needs to perform a redispatch, e.g., due to inaccurate windfarm forecasts. As TSO B has the information about the possible tie-line flows, he can directly incorporate this information in his redispatch optimization, i.e., the inequality $Gp_e \leq g$. In the case of the passive approach, TSO B can guarantee that TSO A will not face congestions as long as TSO B conforms to the deviation limits of the tie-line flows. In the case of the active approach, TSO B can also partially shift the balancing task to TSO A, which will redispatch part of its generation resources. TSO B would have to notify TSO A about the expected tie line flow changes. Due to the inherent linear modeling of power flows in the flexibility set, the calculated flows might differ from the physical flows for large deviations on the tie-lines. Therefore, it is recommended to confirm the feasibility of the proposed remedial action by TSO A using the full power flow equations. The power flow calculation could possibly be done in a distributed way.

TSO A would need to be financially compensated for providing this service. The incurred financial compensation is outside the scope of this paper and is subject of future work.

C. Generalization to Multi-Area

Power flows in a control area might be influenced not only by direct neighboring areas but also by actions taken in control areas further away. This influence becomes even more important when more HVDC interconnections over longer distances are in operation. In this section, we sketch how the described method can be extended to more than two control areas. The iterative algorithm, consisting of four steps, considers n_{TSO} TSOs, where every TSO is responsible for a control area. The iteration is denoted by ν.

1) Every TSO q calculates the projection of the current flexibility set F^q_ν. In the first iteration, the flexibility set consists only of the constraints (2)–(15):

$$F^q_{e,\nu} = \left\{ p^q_e \in \mathbb{R}^{n^q_e} \mid G^q_\nu p^q_e \leq g^q_\nu \right\}. \tag{17}$$

2) The sets $F^q_{e,\nu}$ are exchanged between control areas that are connected via a tie-line or a HVDC interconnection. The

This article has been accepted for inclusion in a future issue of this journal. Content is final as presented, with the exception of pagination.

data exchange can take place bilaterally or via a centralized exchange platform.

3) Every TSO adds the constraints from the neighboring TSOs in the flexibility set. The flexibility set for TSO q, which has m_q neighbors can be written as

$$F_{\nu+1}^q = \left\{ (p_i^q, p_e^q) \in \mathbb{R}^{n_i^q} \times \mathbb{R}^{n_e^q} \middle| \ldots \right.$$
$$\left. \begin{bmatrix} C_{i,N}^q \\ C_{i,N-1}^q \\ 0 \\ \vdots \\ 0 \end{bmatrix} p_i^q + \begin{bmatrix} C_{e,N}^q \\ C_{e,N-1}^q \\ G_{\nu=1}^{q=1} \\ \vdots \\ G_\nu^{q=m_q} \end{bmatrix} p_e^q \leq \begin{bmatrix} b_N^q \\ b_{N-1}^q \\ g_{\nu=1}^{q=1} \\ \vdots \\ g_\nu^{q=m_q} \end{bmatrix} \right\}. \quad (18)$$

Only the parts of $F_{e,\nu}^q$ from the neighbors that actually correspond to tie-lines between the two TSOs in question are integrated.

4) The procedure is repeated for a given number of iterations.

By applying the algorithm in an iterative way, the information on limitations is distributed throughout the network. The number of iterations needed is bounded by the maximum of steps of shortest paths problem between all possible start and end nodes in a graph where a node corresponds to a control area and edges which represent the tie-lines. For the example shown in Fig. 4, in the worst case the number of iterations needed is equal to $n_{\mathrm{TSO}} - 1$.

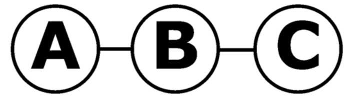

Fig. 4. Illustration of Graph with three TSOs. The algorithm needs a maximum of 2 iterations in order for all TSOs to have all the relevant information.

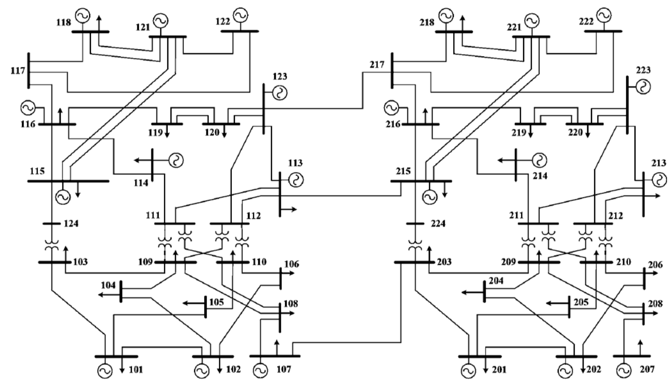

Fig. 5. IEEE RTS96—two-area system. Area A: Buses 1xx. Area B: Buses 2xx.

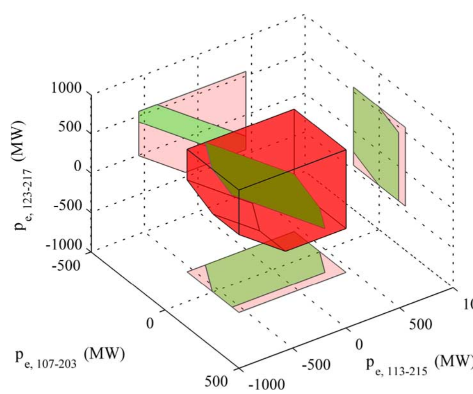

Fig. 6. Result from the Passive (green plane) and Active Approach (red polytope) and corresponding projections on planes orthogonal to the axes. The $\mathrm{N}-1$ criterion is not considered.

VI. Case Studies

We consider the IEEE RTS96 2 area system as depicted in Fig. 5. Area A consists of buses 101 to 123 and area B of buses 201 to 223. The areas are interconnected by three tie-lines and every area is controlled by an individual TSO. For the case study the flexibility set is computed for area A. The loading of the total system is 5700 MW. For simplicity we assume that the TSOs are allowed to redispatch every generation unit in the system.

In the following subsections, we compare the flexibility sets resulting from the *active* and the *passive approach*, with and without the $\mathrm{N}-1$ security criterion, we calculate the exportable flexibility, we compare our approach to the ATC calculation, and we investigate the impact of the permissible local power deviations.

A. Comparison of Methods

Figs. 6 and 7 display the feasible sets of the tie-line deviations given by the resulting polytope $Gp_e \leq g$. In each figure, the active (red) and the passive (green) approach are compared. Fig. 6 shows the case when the $\mathrm{N}-1$ criterion is not considered and Fig. 7 when it is considered. The projections of the feasible sets on the planes spanned by the coordinate axes are shown as well. They represent the feasible combinations of two out of the three tie-lines. In the passive approach, only two of three tie-line flows can be chosen as the third tie-line flow has to be such that the total power exchanged with the neighboring areas remains constant. This is the reason why the polytope of the passive approach is a plane in the 3-D space. For the active approach, TSO A can support region B using redispatch measures and net energy can be exchanged between the areas. Thus the feasible deviations define a larger set than for the passive approach. The additional flexibility of the active approach depends the allowed deviations of the power injections at the different buses. Thus, if the time for ramping is reduced, also the set of the active approach reduces.

Fig. 8 compares the projections from tie-lines 113–215 and 123–217 for both approaches and $\mathrm{N}-1$ and N secure cases. We find the following properties:

- $F_{e,N-1} \subseteq F_{e,N}$, using either the passive or active approach: In order to guarantee the $\mathrm{N}-1$ security criterion, a certain flexibility is reserved.
- $F_{e,\text{passive}} \subseteq F_{e,\text{active}}$, considering either the N or $\mathrm{N}-1$ secure case: The active approach always adds at least as much flexibility as the passive as generation units can be redispatched.
- $F_{e,N-1,\text{passive}} \subseteq F_{e,N,\text{active}}$ holds as logical consequence of the above. But in general it does not hold: $F_{e,N,\text{passive}} \subseteq F_{e,N-1,\text{active}}$

This article has been accepted for inclusion in a future issue of this journal. Content is final as presented, with the exception of pagination.

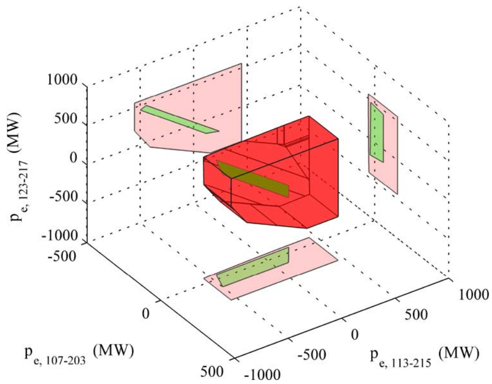

Fig. 7. Result from the Passive (green plane) and Active Approach (red polytope) and corresponding projections on planes orthogonal to the axes. The $\mathrm{N}-1$ criterion is considered.

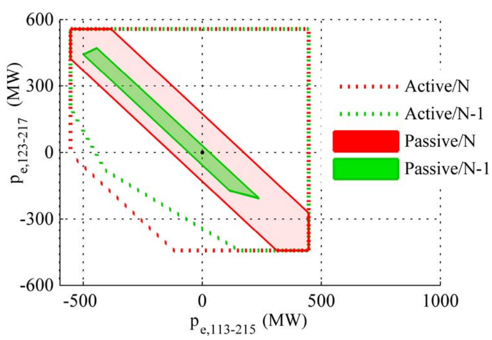

Fig. 8. Comparison of allowed operational states for two tie-lines.

- The origin is always contained in all sets, as the current operating state has to be a feasible solution.

The illustration of up to three tie-lines is convenient, as they can be represented in 3D graphs. However, even for a larger number of tie-lines, the visualization is feasible. One approach is to project the flexibility sets on combinations of two interconnections of interest. Such visualizations could provide valuable information for example in a dispatch control room of a TSO.

B. Exportable Flexibility

In the introduction, we defined the term Exportable Flexibility. This term can only be applied to the active approach, as the passive approach provides flexibility assuming no net power exchange. The amount of flexibility a TSO can provide to its neighbors can be quantified in many different ways. In this work, we provide the range of flexibility that can be accessed by a neighboring TSO. The lower bound of the range is determined by the maximum possible positive and negative deviations that is independent of the location of the disturbance, i.e., independent of the combination of deviations on the tie-lines. The upper bound of the range is calculated as the maximum possible deviation within the given bounds F_e.

For future research it would be interesting to investigate how the exportable flexibility can be transformed into a tradable market product and what metric is most suitable to enable the export of as much flexibility as possible. The ranges for the N-secure and $\mathrm{N}-1$ secure cases are given by the Table I.

We observe that the amount that can be shared independently of the location of the disturbance is relatively limited compared with the maximal possible deviation. On the other hand, this maximal deviation is only feasible for a disturbance which results to tie-line flow deviations in this specific way. We also observe that respecting the $\mathrm{N}-1$ security criterion limits further the exportable flexibility.

TABLE I
RANGES FOR THE N-SECURE AND $\mathrm{N}-1$ SECURE CASES

	Lower bound of range (in MW)	Upper bound of range (in MW)
N secure, negative	-175	-564
N-1 secure, negative	-38	-523
N secure, positive	130	1152
N-1 secure, positive	60	1152

C. Tie-Line Utilization

The available transmission capacity (ATC) indicates the remaining transmission capacity for transfers between two areas [14]. The ATC is selected conservatively, considering numerous possible transactions between two areas as well as a number of relevant congestions [9], [15]. This is necessary as the locations of buses involved in a transaction are generally not known. For the active approach, however, the point of injection of reserves is known and thus also the changes in power flows can be anticipated. Therefore it is expected, that the active approach enables a better tie-line utilization than the case with ATC.

In this case study we focus on the utilization of the tie-lines and determine how much flexibility can be imported and shared for the active case compared with the ATC. It should be noted, that the ATC itself does not quantify the amount of balancing that the generation portfolio of region A can provide to region B but quantifies only how much can be transferred between the areas from a grid perspective. In contrast, the metric determined by the active approach in this paper incorporates both, transmission limits and balancing limits.

The possible power flow deviations on the tie lines in the direction from region A to B that do not exceed the ATC values $\mathrm{ATC}_{B\rightarrow A}$, $\mathrm{ATC}_{A\rightarrow B}$, both larger than zero, are given by the polytope defined by the inequalities

$$\begin{aligned} -\mathrm{ATC}_{B\rightarrow A} \leq \sum p_e \leq \mathrm{ATC}_{A\rightarrow B} \\ \Delta \underline{P}_{L,\mathrm{Tie}} \leq p_e \leq \Delta \overline{P}_{L,\mathrm{Tie}}. \end{aligned} \tag{19}$$

p_e refers again to the flow changes on the tie-lines connecting areas A and B. The tie line flow deviation per line cannot exceed the remaining transmission capacity. The ATC from region A to B as well as from B to A is 120 MW using the calculation method in [15].

We consider two cases for the availability of flexibility in control area A:

- TSO A has full access to all generators in area A and can redispatch them. In other words, after the market clearing the remaining up and down capacities of the generation units serve as reserves to TSO A (Fig. 9).
- TSO A uses only limited amount of the generating capacity in area A. We assume that TSO A is willing to use the manual reserves of only a single generator in area A to support control area B (Fig. 10).

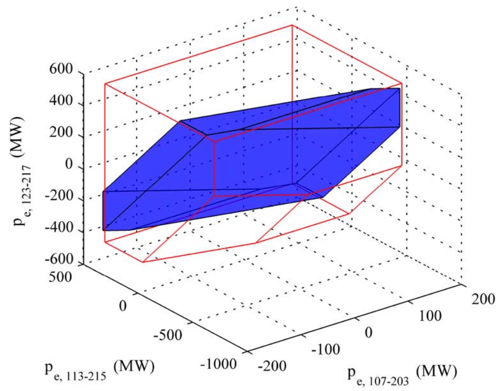

Fig. 9. Comparison of ATC (blue) and resulting polytope of the active approach (red, wired) for full redispatching capabilites in region A.

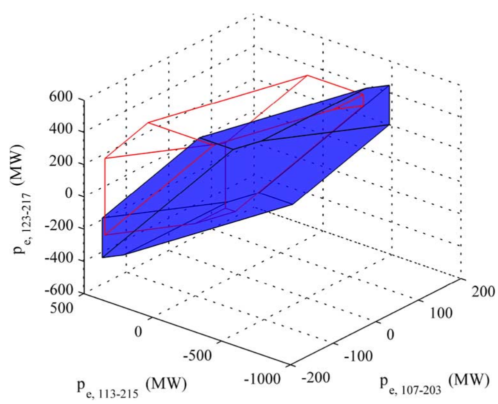

Fig. 10. Comparison of ATC (blue) and resulting polytope of the active approach (red, wired) for limited flexibility available in region A. Parts, where ATC polytope is exceeding the area of the active approach corresponds to combinations, where sufficient transfer capacity but insufficient operational flexibility is available in region A.

Comparing the polytopes resulting from the active approach for the two cases with the polytope for the ATC as shown in Figs. 9 and 10, we observe that in the first case, substantially larger deviations are possible when the active approach is used. But also in the case of limited flexibility in area A, some tie-line flow deviations can be alleviated, that would exceed the calculated ATC. The reason for the improved utilization is the knowledge of the amount and location of available flexibility and the corresponding influence on the power flows a TSO has for his control area. We can conclude, that the active approach enables a less conservative operation of the tie-lines without reducing power system security. But the results of the active approach also depend on the availability and location of flexibility in region A.

It should be noted, that in the parts where the ATC polytope is exceeding the area of the active approach, sufficient ATC would be available for transfers between A and B, but the needed redispatch capabilities in control area A would not be available.

D. Maximum Nodal Variations

In this section, we investigate how the proposed method can mitigate the local deviations arising from for example forecast errors of fluctuating renewable energy sources such as wind or

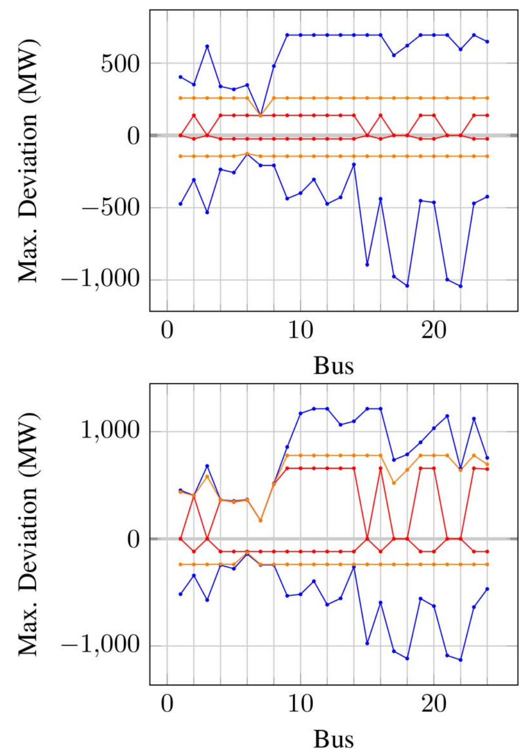

Fig. 11. Maximal possible deviations at buses in region B for active approach (blue) and passive approach (red) and for comparison the ATC case (orange). The upper figure is for a region B with low flexibility (5%), the lower figure for a region B with high flexibility (25%). Positive values correspond to positive deviations, i.e., additional injections, negative values to negative deviations, i.e., additional consumption or reduced production.

PV. We therefore compare the maximum allowed disturbance of every bus in the control area B for the following three cases:

- Passive approach: How large can the disturbance in area B be, without causing a congestion in the neighboring region A?
- Active approach: How large can the disturbance be, when the TSO A helps to compensate the deviation using his procured reserves in area A?
- ATC: For comparison we also consider the case, where control area B can compensate its deviation not only with its own reserves but also has access to reserves in control area A. For the import/export, the ATC has to be respected.

For simplicity, we assume that the reserves in control area B are given as a percentage of the dispatched units in B, e.g., if the reserves are 5%, a generator dispatched with 100 MW provides ± 5 MW of reserves. In region A, the generation units can be fully redispatched. We consider two cases: in the first case, the reserves are 5%, which corresponds to ± 142.5 MW, and in the second case assume a highly flexible system with 25%, which corresponds to ± 712.5 MW of reserves in total. The ATC from region A to B as well as from B to A is 120 MW using the calculation method in [15]. The goal is not to provide absolute values, but rather compare the relative changes for control areas with high and with low inherent flexibility. For simplicity, the N − 1 criterion is not considered for the methods and the ATC calculation. Fig. 11 shows the resulting maximal deviations per bus in area B. The possible deviations are different depending on the bus, but the deviations can become the largest in the case of the active approach. It is obvious, that the deviations can be larger when two areas share their reserves compared to the passive approach. If area B is more flexible, larger deviations can be balanced and the dependence on TSO A is reduced.

VII. Conclusions and Outlook

This paper presented a framework for efficiently characterizing and coordinating available operational flexibility between TSOs. We therefore introduce the term "exportable flexibility", which measures the flexibility that one TSO can offer to its neighbors. The proposed metric takes into account the amount and location of the available reserves, as well as the associated influence on the tie-line flows. The information about this flexibility is calculated through computational geometry and results in a linear matrix inequality that bounds all the feasible tie-line flow deviations. We distinguish between a passive approach, where TSOs are not expected to deviate from their generation schedule to relieve congestions in neighboring areas, and an active approach, where corrective measures from neighboring TSOs are considered. The $\mathrm{N}-1$ security criterion is also included.

Case studies compare the proposed approaches for different system loadings. We show that the active approach enables the export of substantially more flexibility. Especially in the case where the $\mathrm{N}-1$ criterion is considered, the increase in the "exportable flexibility" is between 240%–600% depending on the system loading. The deviations the system can cope with are substantially larger if flexibility is shared between two areas. This allows the incorporation of more intermittent energy sources. A comparison with the ATC also shows, that the active approach allows to improve the tie-line utilization. Future work will focus on a pricing scheme for the exportable flexibility, i.e., pricing the redispatching measures offered to alleviate deviation in neighboring regions. Further, examples focussing on the generalization to more than two areas will be presented.

References

[1] European Parliament, Council, Directive 2009/72/EC of the European Parliament and of the Council of 13 July 2009 Concerning Common Rules for the Internal Market in Electricity and Repealing Directive 2003/54/EC, 2009 [Online]. Available: http://eur-lex.europa.eu/LexUriServ/LexUriServ.do?uri=OJ:L:2009:211:0055:0093:EN:PDF

[2] ENTSO-E Ten-Year Network Development Plan 2010–2020, ENTSO-E, Tech. Rep., 2010 [Online]. Available: https://www.entsoe.eu/index.php?id=232

[3] M. Petersen, K. Edlund, L. Hansen, J. Bendtsen, and J. Stoustrup, "A taxonomy for modeling flexibility and a computationally efficient algorithm for dispatch in smart grids," in *Proc. Amer. Control Conf., American Automatic Control Council*, 2013, pp. 1150–1156.

[4] S. Chatzivasileiadis, T. Krause, and G. Andersson, "Supergrid or local network reinforcements, and the value of controllability—An analytical approach," in *Proc. IEEE Powertech 2013*, Jun. 2013, pp. 1–6.

[5] Y. Makarov, C. Loutan, J. Ma, and P. de Mello, "Operational impacts of wind generation on California power systems," *IEEE Trans. Power Syst.*, vol. 24, no. 2, pp. 1039–1050, May 2009.

[6] K. Trangbaek, M. Petersen, J. Bendtsen, and J. Stoustrup, "Exact power constraints in smart grid control," in *Proc. 2011 50th IEEE Conf. Decision and Control and European Control Conf. (CDC-ECC)*, 2011, pp. 6907–6912.

[7] E. Lannoye, D. Flynn, and M. O'Malley, "Evaluation of power system flexibility," *IEEE Trans. Power Syst.*, vol. 27, no. 2, pp. 922–931, May 2012.

[8] D. Kirschen, J. Ma, V. Silva, and R. Belhomme, "Optimizing the flexibility of a portfolio of generating plants to deal with wind generation," in *Proc. 2011 IEEE Power and Energy Soc. General Meeting*, 2011, pp. 1–7.

[9] R. Christie, B. Wollenberg, and I. Wangensteen, "Transmission management in the deregulated environment," *Proc. IEEE*, vol. 88, no. 2, pp. 170–195, Feb. 2000.

[10] S. Chatzivasileiadis and G. Andersson, "Security constrained OPF incorporating corrective control of HVDC," in *Proc. 14th Power Systems Computation Conf.*, Aug. 2014, pp. 1–8.

[11] W. Y. Ng, "Generalized generation distribution factors for power system security evaluations," *IEEE Trans. Power App. Syst.*, vol. PAS-100, no. 3, pp. 1001–1005, 1981.

[12] M. Herceg, M. Kvasnica, C. Jones, and M. Morari, "Multi-parametric toolbox 3.0," in *Proc. Eur. Control Conf.*, Zürich, Switzerland, Jul. 17–19, 2013, pp. 502–510.

[13] C. N. Jones, E. C. Kerrigan, and J. M. Maciejowski, Equality Set Projection: A New Algorithm for the Projection of Polytopes in Halfspace Representation Dept. Eng., Univ. Cambridge, Cambridge, U.K., Tech. Rep., 2004 [Online]. Available: http://www-control.eng.cam.ac.uk

[14] North American Electric Reliability Council (NERC), Available Transfer Capability Definitions and Determination, 1996 [Online]. Available: http://www.westgov.org/wieb/wind/06-96NERCatc.pdf

[15] G. Ejebe, J. Waight, M. Sanots-Nieto, and W. F. Tinney, "Fast calculation of linear available transfer capability," *IEEE Trans. Power Syst.*, vol. 15, no. 3, pp. 1112–1116, Aug. 2000.

Matthias A. Bucher (S'10) received the B.Sc. and M.Sc. degrees in electrical engineering and information technology from the ETH Zurich, Switzerland, in 2011, where he is currently pursuing the Ph.D. degree.

He is with the Power Systems Laboratory at ETH Zurich. His research interest include modeling and optimization of operational flexibility in power systems.

Spyridon (Spyros) Chatzivasileiadis (S'04–M'14) received the Diploma in electrical and computer engineering from the National Technical University of Athens (NTUA), Greece, in 2007 and the Ph.D. degree from ETH Zurich, Switzerland, in 2013.

He is a postdoc research fellow at Lawrence Berkeley National Laboratory (LBNL), Berkeley, CA, USA. At ETH, he developed methods to integrate high-voltage dc lines (HVDC) in power system planning and operation. In March 2014, he joined the Grid Integration Group at LBNL, where he works on dc microgrids and co-simulation tools to integrate demand response in the distribution and transmission grid.

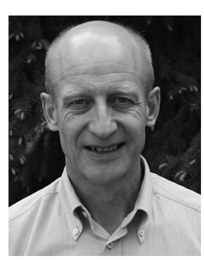

Göran Andersson (M'86–SM'91–F'97) received the M.S. and Ph.D. degrees from the University of Lund, Sweden, in 1975 and 1980, respectively.

In 1980, he joined ASEAs, now ABBs, HVDC division in Ludvika, Sweden, and in 1986, he was appointed full professor in electric power systems at KTH (Royal Institute of Technology), Stockholm, Sweden. Since 2000, he has been a full professor in electric power systems at ETH Zürich (Swiss Federal Institute of Technology), where he also heads the power system laboratory. His research interests include power systems dynamics and control, power markets, and future energy systems.

Dr. Andersson is a fellow of the Royal Swedish Academy of Sciences and of the Royal Swedish Academy of Engineering Sciences. He was the recipient of the IEEE PES Outstanding Power Educator Award 2007 and of the George Montefiore International Award 2010.